"Sunshade World": A fully coupled GCM evaluation of the climatic impacts of geoengineering

D. J. Lunt,[1,2] A. Ridgwell,[1] P. J. Valdes,[1] and A. Seale[1]

Received 15 February 2008; revised 30 April 2008; accepted 15 May 2008; published 25 June 2008.

[1] Sunshade geoengineering - the installation of reflective mirrors between the Earth and the Sun to reduce incoming solar radiation, has been proposed as a mitigative measure to counteract anthropogenic global warming. Although the popular conception is that geoengineering can re-establish a 'natural' pre-industrial climate, such a scheme would itself inevitably lead to climate change, due to the different temporal and spatial forcing of increased CO_2 compared to reduced solar radiation. We investigate the magnitude and nature of this climate change for the first time within a fully coupled General Circulation Model. We find significant cooling of the tropics, warming of high latitudes and related sea ice reduction, a reduction in intensity of the hydrological cycle, reduced ENSO variability, and an increase in Atlantic overturning. However, the changes are small relative to those associated with an unmitigated rise in CO_2 emissions. Other problems such as ocean acidification remain unsolved by sunshade geoengineering. **Citation:** Lunt, D. J., A. Ridgwell, P. J. Valdes, and A. Seale (2008), ''Sunshade World'': A fully coupled GCM evaluation of the climatic impacts of geoengineering, *Geophys. Res. Lett.*, *35*, L12710, doi:10.1029/2008GL033674.

1. Introduction

[2] Geoengineering can be defined as the ''intentional large-scale manipulation of the environment'' [*Keith*, 2000] and has been considered for the mitigation of climate change in response to elevated anthropogenic greenhouse gas emissions [*Intergovernmental Panel on Climate Change* (*IPCC*), 2007]. Various schemes have been proposed, including the injection of sulphate aerosols into the atmosphere [*Crutzen*, 2006] and increasing carbon sinks through oceanic iron fertilisation [*Martin*, 1990]. *Early* [1989] proposed the implementation of a space-based ''sunshade'', situated at the Lagrange point (L1) between the Earth and the Sun, designed to reduce solar insolation. The feasibility of such a sunshade was assessed by *Angel* [2006], who concluded that it could be developed and deployed in about 25 years at a cost of a few trillion dollars, while others have assessed ethical considerations [e.g., *Jamieson*, 1996; *Bodansky*, 1996]. Here we focus on the climatic impacts of sunshade geoengineering.

[3] The purpose of sunshade geoengineering is to reduce the incident solar radiation at the top of the atmosphere, in order to offset the surface warming caused by increased atmospheric greenhouse gas concentrations. However, although the global annual mean temperature could in theory be reduced to exactly that characterising pre-industrial climate, the differing spatial and temporal distributions of the solar and CO_2 forcings would result in residual differences in climate between the ''Sunshade World' and pre-industrial. In this study, we calculate the nature and magnitude of this residual climate change.

[4] Analogous experiments have been carried out previously by *Govindasamy and Caldeira* [2000], *Govindasamy et al.* [2003] (hereinafter referred to as G2003), and *Matthews and Caldeira* [2007]. However, all these studies were carried out with models of reduced complexity. *Govindasamy and Caldeira* [2000] and G2003 used a full complexity atmospheric model, but in conjunction with a 'slab' ocean, which is not capable of predicting changes in ocean circulation and heat transport, and includes a relatively simple representation of sea ice. *Matthews and Caldeira* [2007] used a fully coupled atmosphere-ocean model, but with a reduced complexity (energy-moisture balance, EMB) atmosphere. Although atmospheric EMB models provide useful insights into spatial distributions of temperature change and timescales of response of the system to perturbations, they are not capable of representing changes in atmospheric circulation and moisture transport [*Weaver et al.*, 2001]. Both *Govindasamy and Caldeira* [2000] and G2003 recommended that future work should be carried out using models which have a fully coupled and dynamic representation of oceans and sea ice, and associated feedbacks. This is the challenge which we address here.

2. Experimental Design

[5] We use the fully coupled atmosphere-ocean UK Met Office GCM, HadCM3L [*Cox et al.*, 2000]. HadCM3L has a horizontal resolution of 3.75° longitude by 2.5° latitude in the atmosphere and ocean, 19 vertical levels in the atmosphere and 20 vertical levels in the ocean. It consists of a hydrostatic primitive-equation atmosphere, with parameterisations for subgridscale processes such as convection [*Gregory and Rowntree*, 1990]. The ocean includes parameterisations of eddy mixing [*Gent and McWilliams*, 1990], and a dynamic-thermodynamic sea ice scheme [*Cattle and Crossley*, 1995]. The configuration of the model is identical to that described by *Lunt et al.* [2007], except that we use a more recent version of the land-surface scheme (MOSES2.2), with fixed prescribed modern vegetation.

[6] We carried out three 220-year simulations, all initialised from the end of a spin-up totaling more than 1000 years. The first is a pre-industrial control (*Pre*), the second has atmospheric CO_2 set at 1120 ppmv, 4× the pre-industrial

[1] BRIDGE, School of Geographical Sciences, University of Bristol, Bristol, UK.
[2] Geological Sciences Division, British Antarctic Survey, Cambridge, UK.

0094-8276/08/2008GL033674$05.00

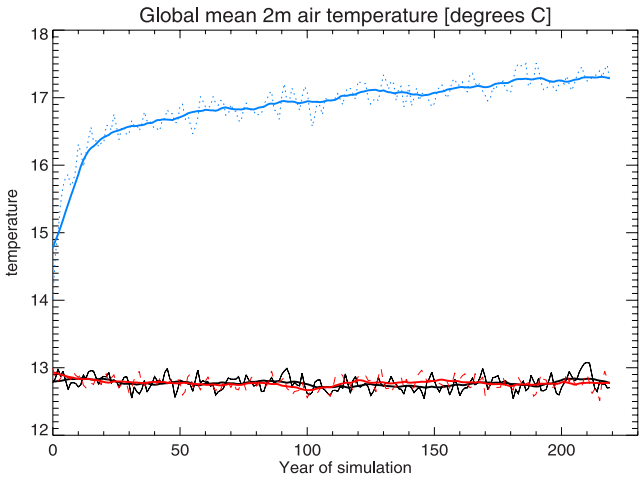

Figure 1. Time series of global annual mean 2 m air temperature in simulations *Pre* (black solid), *Fut* (blue dotted), and *Geo* (red dashed). Thick line represents a 20-year running mean.

value (*Fut*), and the third has 4 × CO_2 and a reduced solar constant (*Geo*). In simulation *Geo*, we reduced the solar constant such that the global annual mean 2 m air temperature was as close as possible to that of the *Pre* simulation. This was achieved by first carrying out a preparatory simulation with a first estimate for the required reduction. This was refined twice by assuming a linear relation between applied forcing and surface temperature change. As a result, simulation *Geo* has a solar constant 57 Wm^{-2} less than that of *Pre*, a reduction of 4.2%. For comparison, G2003 found that they required a reduction of 3.6% to offset a 4× increase in CO_2.

[7] The time series of global annual mean 2 m air temperature (T_{2m}) in simulations *Pre*, *Geo* and *Fut* is shown in Figure 1. In the following sections, the results of the last 60 years of these simulations are described and discussed. Over this period, the average of T_{2m} is 12.78°C in simulation *Pre*, 12.77°C in simulation *Geo*, and 17.24°C in simulation *Fut*. The close agreement in T_{2m} between the *Pre* and *Geo* values (0.01°C) compares with a difference of 0.07°C obtained by G2003. The standard deviation of T_{2m} over this period is about 0.1°C in the GCM simulations. We have thus produced a climate that is indistinguishable from pre-industrial when viewed from the widely used metric of global mean surface air temperature.

3. Results

[8] The 1-dimensional energy balance structure of the Sunshade World is rather different to that of the pre-industrial. At the top of the atmosphere, the applied decrease in incoming solar radiation (14.2 Wm^{-2}) is balanced by a reduction in outgoing solar radiation (6.8 Wm^{-2}, of which 4.2 Wm^{-2} is a direct result of the decreased incoming solar radiation, and 2.6 Wm^{-2} is due to a decrease in planetary albedo), and a decrease in outgoing long wave radiation (7.5 Wm^{-2}). The decrease in outgoing long wave radiation is due to a colder upper atmosphere in the geoengineered world, due largely to the increased tropospheric CO_2. At the surface, the decrease in downwards solar radiation (5.5 Wm^{-2}) is balanced largely by a decrease in latent heat of evaporation (4.4 Wm^{-2}), and a decrease in upwards solar radiation (0.9 Wm^{-2}, of which 0.7 Wm^{-2} is a direct result of the decreased downward solar radiation, and 0.2 Wm^{-2} is due to a decrease in surface albedo). The decrease in latent heat is related to a cooler tropical ocean in the geoengineered climate (see below).

[9] Although we have tuned the solar constant in simulation *Geo* so that the value of T_{2m} is near identical to that of *Pre*, climate differs markedly regionally between the two simulations. For example, there is a warming in surface air temperature at high latitudes in *Geo* compared to *Pre*, and a cooling in the tropics (Figure 2a). This is due to the fact that a percentage reduction in solar insolation leads to a latitudinal distribution of absolute solar forcing due to the curvature of the Earth, with greater forcing towards the equator, and less towards the poles. The 4.2% reduction applied leads to an annual mean TOA forcing of −17 Wm^{-2} at the equator and −7 Wm^{-2} at both poles. However, the forcing due to the increased atmospheric CO_2 in simulation *Geo* does not have the same latitudinal structure. It is greatest at the equator and less at high latitudes, but the latitudinal gradient is less steep than for the solar forcing, and not symmetric across the equator, with a minimum over Antarctica [*Forster et al.*, 2000]. Combining the solar and CO_2 forcing gives a negative forcing at the equator, and a positive forcing at the poles. This is reflected in the surface air temperature response. Spatially, 74% of the annual mean temperature changes are statistically significant at a 95% confidence limit, as given by a Student t-test (Figure 2a), in comparison with 24% in G2003. Some of this difference is likely due the greater length of averaging period in our simulation (60 years, compared with 15 years given by G2003).

[10] The temperature response is not directly proportional to the applied forcing, due to non-linear amplification of the forcing by positive feedbacks in the system, and a redistribution of heat due to changes in atmospheric and ocean circulation. The maximum increase in surface temperature is in the Beaufort and East Siberian Seas, north of Alaska and Siberia, which is associated with a decrease in sea ice (Figure 2b). The maximum decrease in surface air temperature occurs in the south east Atlantic, off the west coast of Angola and Namibia. Here, the amplified signal is due to an increase in upwelling, and shoaling of the thermocline in the tropics. As expected, the poleward heat transport in both hemispheres is reduced due to the decreased meridional temperature gradient; changes to the atmospheric heat transports (maximum of 0.18 PW) dominate over changes to the ocean heat transport (maximum of 0.09 PW).

[11] Another interesting impact of the sunshade is a slight decrease in temperature in the Barents Sea. In the *Pre* simulation, this region is kept relatively warm due the presence of the wind-driven North Atlantic drift. In simulation *Geo*, there is a reduction in the intensity of this current, which results in a cooling in the Barents Sea, associated with a slight increase in sea ice.

[12] As well as spatial differences, there are temporal differences between the temperature in Sunshade World and pre-industrial. There is a reduction in the amplitude of the seasonal cycle; the seasonal temperature range (Northern Hemisphere, JJA minus DJF) decreases by 0.3°C in the

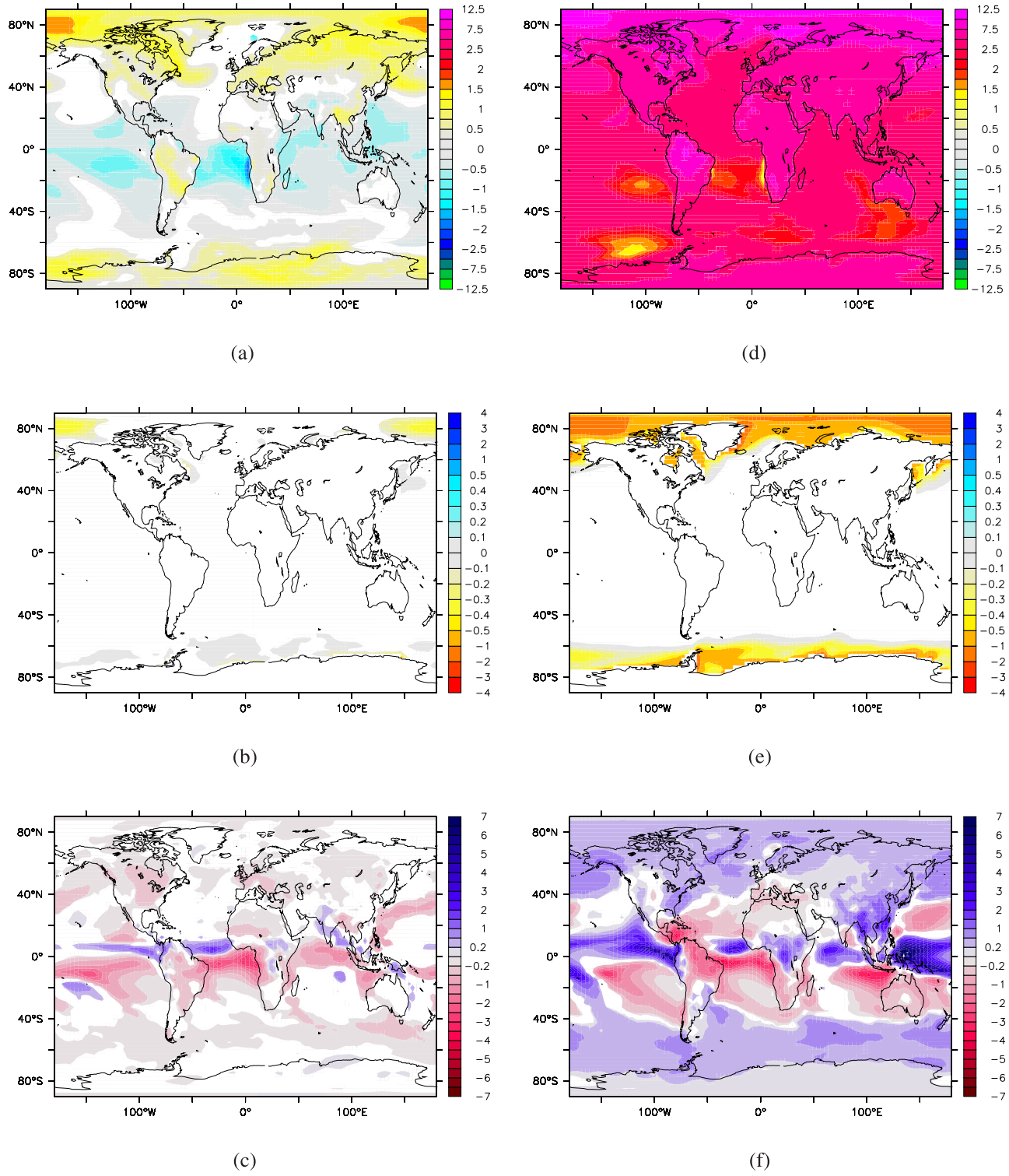

Figure 2. (left) Change in climatic parameters in Sunshade World relative to pre-industrial: (a) 2 m air temperature (°C), (b) sea ice depth (m), and (c) precipitation (mmday^{-1}). (right) Change in climatic parameters in the 4 × CO_2 world relative to pre-industrial: (d) 2 m air temperature (°C), (e) sea ice depth (m), and (f) precipitation (mmday^{-1}). Regions where the difference is not statistically significant at a 95% confidence limit, as given by a Student T test, are masked out in white.

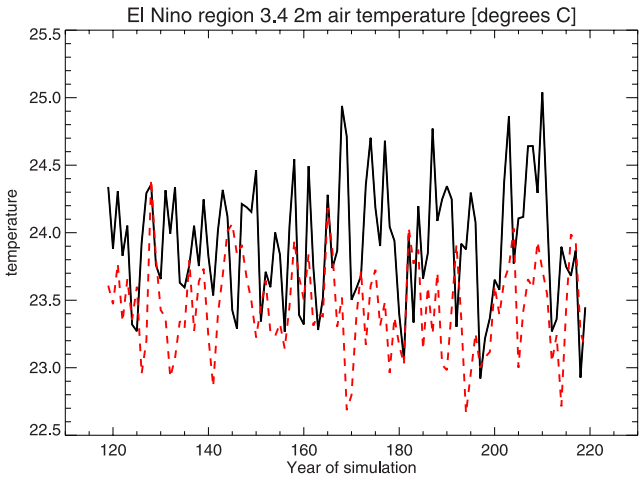

Figure 3. Time series of annual mean 2 m air temperature in El Niño region 3.4 in simulations *Pre* (black solid) and *Geo* (red dashed).

tropics, 0.4°C in the subtropics and mid latitudes, and 1.5°C in the high latitudes relative to pre-industrial. This is because the applied solar forcing has a strong seasonal component (see G2003, Figure 1 bottom panel), which acts in a direction so as to reduce seasonality, whereas the balancing due to the increase in CO_2 is more stable throughout the year. We do not simulate a large change in the amplitude of the global mean diurnal cycle in simulation *Geo* relative to *Pre*, in agreement with G2003; however, in dry regions such as the Gobi and Sahara deserts, there are reductions in diurnal cycle up to 1.5°C.

[13] We also find important differences in the hydrological cycle, with Sunshade World generally drier than the pre-industrial (Figure 2c). The global annual mean precipitation decreases by 5%; the largest absolute decreases are in the tropics, and are related to the cooler and therefore less evaporative tropical surface ocean. However, a northwards shift of the ITCZ, associated with the decreased meridional temperature gradient, leads to increased precipitation just north of the equator in the Atlantic and eastern Pacific. Despite this reduction in meridional temperature gradient, and an associated decrease in the intensity of the northern Pacific storm track, the large scale precipitation changes in mid and high latitudes are small. Perhaps counter-intuitively, the decreased precipitation in the tropics does not lead to a decrease in soil moisture. Because evaporation also decreases due to the lowered surface temperature, there is in fact a small increase in soil moisture. So the decreased precipitation may not be likely to have a detrimental effect on food production in the tropics. The less intensive hydrological cycle also leads to an almost global decrease in low and medium-level stratiform cloud, and the convective cloud cover change is similar to that of tropical precipitation.

[14] The dynamic ocean component of HadCM3L allows us to assess possible impacts on ENSO of the geoengineered climate due to the reduction of insolation in the tropics. Figure 3 shows a time series of surface air temperature in El Niño region 3.4, in the preindustrial and Sunshade World. The expected reduction in annual mean temperature is apparent in the geoengineered time series, but there is also a decrease in the variability. The standard deviation is 0.46°C in simulation *Pre* and 0.35°C in simulation *Geo*. Wavelet analysis of the two time series does not indicate a significant shift in the dominant ENSO timescale. The decrease in the intensity of the ENSO signal is most likely due to the cooler tropical SSTs and associated reduced tropical convection. This reduces the strength of the positive feedback which in *Pre* acts to intensify El Niño events by increasing the strength of Walker circulation and further amplifying the tropical SST anomaly.

[15] We have also assessed the response of the density-driven thermohaline circulation to the sunshade geoengineering. In many of the future climate GCM simulations reported by the IPCC, there is a reduction in the strength of the Atlantic MOC (Meridional Overturning Circulation) relative to pre-industrial [*IPCC*, 2007]. This feature is also predicted in our *Fut* simulation, with a maximum reduction of 5 Sv (for comparison, the maximum overturning in the *Pre* simulation is about 18 Sv). The main causes of this are an increase in high latitude precipitation in the warmer climate, and warmer SSTs, which reduce the density of the surface waters in the North Atlantic, resulting in decreased overturning. In contrast, we find that the circulation in simulation *Geo* is characterised by a slight increase in overturning (maximum 1.6 Sv) compared to pre-industrial, due to a reduction in northwards moisture transport due to the cooler tropics. The impact of the sunshade thus has the opposite effect to the CO_2 forcing, and tends to stabilise rather than destabilise the Atlantic MOC.

4. Discussion

[16] Although HadCM3L has been used in many studies of future and paleo climates [e.g., *Cox et al.*, 2000; *Lunt et al.*, 2007], it has reduced resolution compared to the most recent version (HadGEM) of the UK Met Office used in the recent IPCC assessment report [*IPCC*, 2007], and therefore can no longer be considered a 'state of the art' GCM. We use HadCM3L here because of its relative computational efficiency. *Collins* [2000] found different ENSO responses to CO_2 in two different versions of the UK Met Office model, which he attributed to differences in the physical parameterisation schemes. Therefore, some of the ENSO-related results discussed in this paper may be model-dependent, and should be verified with other models.

[17] We have kept vegetation fixed at pre-industrial values throughout all the simulations, thereby neglecting vegetation-climate feedbacks. It is possible that the high CO_2 in a geoengineered world would lead to increased global NPP by CO_2 fertilisation [*Govindasamy et al.*, 2002], although recent work has suggested that this process may be limited by nutrient availability [*Thornton et al.*, 2007]. Furthermore, high CO_2 may lead to shifts in vegetation type due to CO_2 controls on competition between plants with C_4 and C_3 photosynthetic pathways [*Ehleringer et al.*, 1997]. However, future vegetation changes are likely to be dominated by anthropogenic land-use change - a factor we cannot predict with any confidence. We have therefore chosen to keep all vegetation characteristics fixed.

[18] It should be noted that the stratospheric response of the model is somewhat uncertain, due to the low vertical resolution in the upper atmosphere, and the fact that we have neglected potential positive feedbacks involving ozone

and polar stratospheric clouds, which could act to decrease the stratospheric temperature still further in the Sunshade World (G2003).

5. Conclusions

[19] To our knowledge, this is the first analysis of sunshade geoengineering using a complex GCM with a fully coupled atmosphere and dynamic ocean, an analysis that could also be applied to injection of sulphate aerosols into the upper atmosphere. Compared to the pre-industrial, we find that a sunshade geoengineered world with an identical global annual mean surface temperature has a reduced meridional temperature gradient, and cooler tropics. There is a reduction in the intensity of the hydrological cycle, in particular in tropical regions. This is all in agreement with previous work from a slab ocean model (G2003). In addition, we simulate a significant decrease in Arctic sea ice in the sunshade geoengineered world, and a decrease in temperature seasonality relative to pre-industrial. Furthermore, the use of a fully dynamic ocean in this study allows analysis of the ENSO and thermohaline circulation of the geoengineered climate - we find a reduction in the amplitude of ENSO, and a slight increase in the strength of the Atlantic MOC, relative to pre-industrial.

[20] Despite significant differences in temperature and sea ice in *Geo* relative to the pre-industrial, compared to *Fut* (Figures 2d and 2e) the predicted changes are relatively small. *Fut* is globally 4.5°C warmer than *Pre*, and 8.8°C warmer at high latitudes; for comparison, *Geo* is 0.8°C warmer at high latitudes. Similarly, although we find significant decreases in precipitation in *Geo*, they are small compared to the precipitation changes associated with the warmer climate of *Fut* (Figure 2f). In this respect, we find that the sunshade geoengineering is highly successful. However, other direct effects of increased CO_2 remain unmitigated, in particular ocean acidification and the subsequent impact on ecosystems. Because of this, we can not recommend sunshade geoengineering as an alternative to the reduction of emissions. This is even before the high cost, and possible ethical considerations, of a sunshade geoengineering scheme have been considered.

[21] Finally, it is interesting to note that the combination of reduced solar forcing and high CO_2 has been present before, in the geological past. The reduction in solar constant of 4.2% (57 Wm^{-2}) is similar to that of the Cambrian, 500 million years ago [*Gough*, 1981]; at this time, it is also likely that CO_2 levels were higher than pre-industrial [*Royer*, 2006]. Therefore, geoengineering a future climate - Sunshade World - characterised by reduced solar forcing and elevated CO_2, in terms of the gross radiation balance could be likened to turning the clock back to the Cambrian World.

[22] **Acknowledgments.** This work was carried out in the framework of the British Antarctic Survey GEACEP (Greenhouse to ice-house: Evolution of the Antarctic Cryosphere And Palaeoenvironment) programme. DJL is also part-funded by an RCUK (Research Councils UK) Fellowship. AJR is funded by the Royal Society. The authors would like to thank two anonymous reviewers who provided constructive comments and David A. Richards at the University of Bristol, UK for advice on improving the quality of the figures.

References

Angel, R. (2006), Feasibility of cooling the Earth with a cloud of small spacecraft near the inner Lagrange point (L1), *Proc. Natl. Acad. Sci., U. S. A.*, *103*, 17,184–17,189.

Bodansky, D. (1996), May we engineer the climate?, *Clim. Change*, *33*, 309–321.

Cattle, H., and J. Crossley (1995), Modelling Arctic climate change, *Philos. Trans. R. Soc. London, Ser. A*, *352*, 201–213.

Collins, M. (2000), Understanding uncertainties in the response of ENSO to greenhouse warming, *Geophys. Res. Lett.*, *27*, 3509–3512.

Cox, P. M., R. A. Betts, C. D. Jones, S. A. Spall, and I. J. Totterdell (2000), Acceleration of global warming due to carbon-cycle feedbacks in a coupled climate model, *Nature*, *408*, 184–187.

Crutzen, P. (2006), Albedo enhancement by stratospheric sulphur injections: A contribution to resolve a policy dilemma?, *Clim. Change*, *77*, 211–219.

Early, J. T. (1989), Space-based solar screen to offset the greenhouse effect, *J. Br. Interplanet. Soc.*, *42*, 567–569.

Ehleringer, J. R., T. E. Cerling, and B. R. Helliker (1997), C_4 photosynthesis, atmospheric CO_2 and climate, *Oecologia*, *112*, 285–299.

Forster, P. M., M. Blackburn, R. Glover, and K. P. Shine (2000), An examination of climate sensitivity for idealised climate change experiments in an intermediate general circulation model, *Clim. Dyn.*, *16*, 833–849.

Gent, P. R., and J. C. McWilliams (1990), Isopycnal mixing in ocean circulation models, *J. Phys. Oceanogr.*, *20*, 150–155.

Gough, D. O. (1981), Solar interior structure and luminosity variations, *Sol. Phys.*, *74*, 21–34.

Govindasamy, B., and K. Caldeira (2000), Geoengineering Earth's radiation balance to mitigate CO_2-induced climate change, *Geophys. Res. Lett.*, *27*, 2141–2144.

Govindasamy, B., S. Thompson, P. B. Duffy, K. Caldeira, and C. Delire (2002), Impact of schemes on the terrestrial biosphere, *Geophys. Res. Lett.*, *29*(22), 2061, doi:10.1029/2002GL015911.

Govindasamy, B., K. Caldeira, and P. B. Duffy (2003), Geoengineering Earth's radiation balance to mitigate climate change from a quadrupling of CO_2, *Global Planet. Change*, *37*, 157–168.

Gregory, D., and P. R. Rowntree (1990), A mass flux convection scheme with representation of cloud ensemble characteristics and stability-dependent closure, *Mon. Weather Rev.*, *118*, 1483–1506.

Intergovernmental Panel on Climate Change (IPCC) (2007), *Climate Change 2007: The Physical Science Basis. Contribution of Working Group I to the Fourth Assessment Report of the Intergovernmental Panel on Climate Change*, edited by S. Solomon et al., Cambridge Univ. Press, Cambridge, U. K.

Jamieson, D. (1996), Ethics and intentional climate change, *Clim. Change*, *33*, 323–336.

Keith, D. W. (2000), Geoengineering the climate: History and prospect, *Annu. Rev. Energy Environ.*, *25*, 245–284.

Lunt, D. J., I. Ross, P. J. Hopley, and P. J. Valdes (2007), Modelling late Oligocene C_4 grasses and climate, *Palaeogeogr. Palaeoclimatol. Palaeoecol.*, *251*, 239–253.

Martin, J. H. (1990), Glacial-interglacial CO_2 change: The iron hypothesis, *Paleoceanography*, *5*, 1–13.

Matthews, H. D., and K. Caldeira (2007), Transient climate-carbon simulations of planetary geoengineering, *Proc. Natl. Acad. Sci. U. S. A.*, *104*, 9949–9954.

Royer, D. L. (2006), CO_2-forced climate thresholds during the Phanerozoic, *Geochim. Cosmochim. Acta*, *70*, 5665–5675.

Thornton, P. E., J.-F. Lamarque, N. A. Rosenbloom, and N. M. Mahowald (2007), Influence of carbon-nitrogen cycle coupling on land model response to CO_2 fertilization and climate variability, *Global Biogeochem. Cycles*, *21*, GB4018, doi:10.1029/2006GB002868.

Weaver, A. J., et al. (2001), The UVic Earth System Climate Model: Model description, climatology and application to past, present and future climates, *Atmos. Ocean*, *39*, 361–428.

D. J. Lunt, A. Ridgwell, A. Seale, and P. J. Valdes, School of Geographical Sciences, University of Bristol, Bristol, BS8 1SS, UK. (d.j.lunt@bristol.ac.uk)